A Collimated Surface-Wave-Excited High-Impedance Surface Leaky-Wave Antenna

Zi Long Ma, *Member, IEEE*, Chi Hou Chan, *Fellow, IEEE*, Kung Bo Ng, *Member, IEEE*, and Li Jun Jiang, *Senior Member, IEEE*

***Abstract*—This letter presents a novel high-impedance surface (HIS)-based leaky-wave antenna excited by collimated surface wave (SW). The proposed antenna consists of two identical SW launchers (SWLs) and an HIS structure. Regarding the SWL, it is based on an offset-fed parabolic reflector. By using the substrate-integrated waveguide technique, the reflector system is integrated in the planar substrate. For the HIS, it is formed by a periodically arranged rectangular microstrip patch array. The proposed SWL can generate collimated SW with the TM_0 propagation mode. With the perturbation of the HIS, the guided SW can be transformed to $m = -1$ space-harmonic-mode leaky wave. In addition, in order to obtain efficient broadside radiation, an additional secondary slit is properly designed in each unit cell of the HIS to suppress the open-stopband effect. A prototype of the proposed antenna is demonstrated by both full-wave simulation and experimental verification. Continuous beam scan can be realized from -36° to $+35.5^\circ$ within the frequency range of 16–22 GHz.**

***Index Terms*—Collimated wave, high-impedance surface (HIS), leaky wave, surface wave (SW).**

I. Introduction

SURFACE waves (SWs) are those waves that are bound to a surface or an open interface between two materials (dielectric, metal, free space, and so on) [1]. In the past decades, the manipulation of SWs has received much interest in the electromagnetics community. Substantial efforts have been dedicated to control the SWs to realize efficient radiation. In order to efficiently excite SW on a grounded substrate, two SW launchers (SWLs) were studied in [2] and [3]. Both of the designs are based on slot configuration and employ the principle of the Yagi–Uda antenna to achieve good directive performance. By employing the SWL presented in [3], a type of SW-excited leaky-wave antenna was proposed in [4] and [5]. In the designs of this kind of antenna, periodic grating-like metal strips were employed to act as the radiating surface. The bounded TM_0-mode SW can be perturbed by the strips and transformed to the leaky-wave radiation mode. However, because of the intrinsic resonant nature of the Yagi–Uda-type SWLs, most of the existing designs are difficult to achieve wideband performance. Within their operating bands, the radiation patterns and antenna gain often have relatively large variations.

In this letter, we propose a novel collimated SW-excited high-impedance-surface (HIS) leaky-wave antenna. Different from the previous studies, we propose a 2-D offset-fed parabolic reflector-based SWL. It applies the substrate-integrated waveguide (SIW) technique, and the entire reflector system is integrated in a planar substrate. By proper design, it can create a collimated TM_0 SW mode (consistent with the TEM mode). On the other hand, a periodically arranged rectangular microstrip patch array is designed in this letter as well. It plays the role of a radiating surface. As we know, leaky-wave antennas often have features of frequency-based beam scanning [6]. However, some of them based on periodic structures often have to face the open-stopband effect. At the broadside radiation frequency, a stopband appears and the radiation performance drops substantially. In order to suppress this effect, we design a secondary slit in each unit cell of the HIS. This method is inspired by the work of [7] and [8]. Through the study, it is found that the proposed antenna has wideband performance. In the operating band, the radiation patterns are stable and the gain variation is small. Continuous beam scan through the broadside direction can be realized. The proposed antenna has the features of low cost, low profile, and ease of fabrication. It can be applied to various radar systems and satellite communications. This letter is organized as follows. In Section II, the proposed antenna configuration, the operation, and design principles are introduced. The experimental and numerical results are presented, compared, and discussed in Section III. Finally, a conclusion can be found in Section IV.

II. Antenna Design

The overall configuration of the proposed antenna is presented in Fig. 1(a). We can see that the antenna consists of two identical SWLs and a periodic HIS structure. The antenna is fed from Port 1 on the left side, while the SWL on the right-hand side is used to reduce the endfire radiation. In the practical implementation, a matched 50-Ω load is connected to Port 2. Fig. 1(b) shows

Manuscript received January 20, 2017; revised April 3, 2017; accepted April 13, 2017. Date of publication April 24, 2017; date of current version July 31, 2017. This work was supported in part by the Research Grants Council of Hong Kong under Grant ITP/045/14LP, CityU Grant 110713, the NSFC under Grant 61271158, HKU Seed Fund 201309160052, and CityU Grant SKLMW 9360130. *(Corresponding author: Zi Long Ma.)*

Z. L. Ma was with the University of Hong Kong, Hong Kong. He is now with the State Key Laboratory of Millimeter Waves, City University of Hong Kong, Hong Kong (e-mail: mazilong@connect.hku.hk).

C. H. Chan and K. B. Ng are with the State Key Laboratory of Millimeter Waves, City University of Hong Kong, Hong Kong (e-mail: eechic@cityu.edu.hk; kubong@cityu.edu.hk).

L. J. Jiang is with the Department of Electrical and Electronic Engineering, The University of Hong Kong, Hong Kong (e-mail: ljiang@eee.hku.hk).

Color versions of one or more of the figures in this letter are available online at http://ieeexplore.ieee.org.

Digital Object Identifier 10.1109/LAWP.2017.2696302

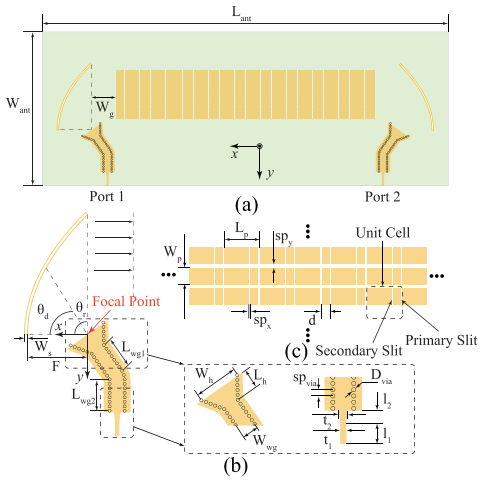

Fig. 1. Configuration of the proposed collimated SW-excited HIS leaky-wave antenna. The orange and green colors indicate metal and dielectric substrate, respectively. (a) Full view of the proposed antenna with the coordinate system. (b) Top view of the proposed SWL and structure details. (c) Proposed HIS structure and illustration of unit cell. $L_{\text{ant}} = 248.4$, $W_{\text{ant}} = 94$, $W_g = 15$, $W_s = 1$, $L_{wg1} = 10.5$, $L_{wg2} = 10.5$, $W_h = 13$, $L_h = 6$, $W_{wg} = 5$, $sp_{\text{via}} = 1.5$, $D_{\text{via}} = 1$, $t_1 = 1.5$, $t_2 = 2.2$, $l_1 = 5$, $l_2 = 3$, $W_p = 2.5$, $L_p = 5.3$, $sp_x = 0.3$, and $sp_y = 0.5$ (in mm). $\theta_r = 90^\circ$ and $\theta_d = 35^\circ$.

the detailed geometry of the proposed SWL. It can be seen that the SWL is formed by an offset-fed parabolic reflector system. The reflector part is directly carved from the dielectric substrate. The four walls are metallized by copper. An SIW-based planar horn is adopted as the feed. After the port, a linearly tapered microstrip line is designed to provide a smooth transition to the SIW part. In Fig. 1(c), the configuration of the HIS structure is presented. It is implemented by a linearly arranged rectangular microstrip patch array. The black dashed line indicates the unit cell. It can be seen that, other than the primary slits that are formed by the microstrip array, a secondary slit is added on each of the patches as well. In this letter, a prototype of the proposed antenna with a 10 × 30 microstrip array (300 unit cells) is designed for demonstration. It is worth mentioning that since the offset-fed parabolic reflector system is adopted as the SWL in this design, the proposed antenna may have longer geometry than the other existing leaky-wave configurations. On the other hand, it should be mentioned that the selection of dielectric substrate is important in this design. As described in [9], a thicker substrate and higher dielectric constant will be easier to generate SWs. Thus, a 75-mil-thick Rogers 6010 laminate with a dielectric constant equals to 10.2 is chosen in our design. The loss tangent is 0.0023.

A. Design of the SWL

The parabolic reflector surface can be described by

$$\begin{cases} x_p = \frac{2F}{1+\sin\theta_p}\sin\theta_p \\ y_p = \frac{2F}{1+\sin\theta_p}\cos\theta_p \end{cases} \quad (1)$$

where p stands for an arbitrary point on the reflector surface, x_p and y_p are the positions of point p, θ_p refers to the angle from the x-axis, and F is the focal length. The design principle of the proposed SWL is similar to the conventional offset parabolic

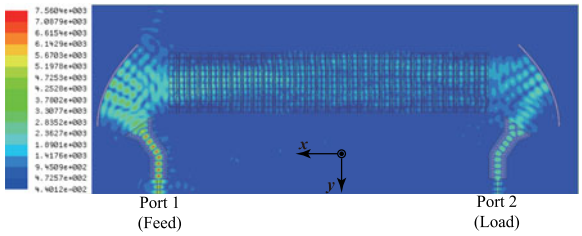

Fig. 2. Full-wave simulated E-field distribution of the proposed antenna (Unit: V/m).

reflectors, which can be found from [10]. In this letter, the size of the reflector surface is determined according to the physical dimension of the HIS along the y-axis to provide a large enough illumination aperture, as shown in Fig. 2. We can see that almost all the HIS unit cells in the y-direction are illuminated by the excited SW. For the SIW structure, the width W_{wg} is selected to propagate the fundamental TE mode. The L_{wg1} and L_{wg2} should be designed as short as possible to reduce the unnecessary power loss. The design principle of other SIW parameters, like the via diameter and spacing, is identical to that of the conventional SIW [11].

B. Design of the HIS

Based on the Bloch–Floquet theory, we can find out the expression of the dispersion relation of the periodic HIS

$$\beta_m(\omega) = \pm\left[\beta_{\text{sw}}(\omega) + \frac{2m\pi}{L_p}\right], \quad m = 0, \pm1, \pm2, \pm3... \quad (2)$$

where β_{sw} stands for the phase constant of the fundamental SW. For the proposed antenna, the $m = -1$ space harmonic mode is excited to realize leaky-wave radiation. The main beam direction θ (angle from broadside direction) can be approximated by

$$\theta \approx \sin^{-1}(\beta_{-1}(\omega)/k_0). \quad (3)$$

From the derivations listed above, it can be seen that the physical length of the unit cell dominates the operation frequency and the beam angle. We can properly change L_p to make the antenna meet the requirements of frequency and beam direction. Since the HIS shows partially reflective properties, the parameters W_p and sp_y are tuned to achieve good impedance matching. Through the study, it is found that a large W_p and a small sp_y will lead to impedance mismatch. In addition, a large value of the parameter sp_x will slightly increase the antenna gain. However, this parameter should be carefully selected because a large sp_x will be difficult to implement in the unit cell. Improper design of sp_x will lead to overlap of the primary and secondary slits.

If we only employ the rectangular microstrip patches as the radiating surface without the additional secondary slits, the open-stopband phenomenon will appear. In Fig. 3, the dashed lines show the magnitudes of S_{11} and S_{21} of the configuration without the secondary slits. It can be seen that an obvious stopband appears from 17.6 to 19 GHz. The magnitude of S_{11} is higher than -10 dB within this range. At the same time, Fig. 4 presents the simulated radiation patterns around the broadside direction.

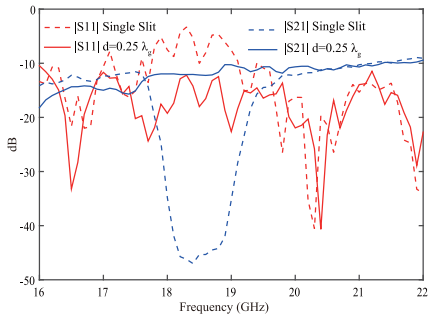

Fig. 3. Simulated S-parameters with open-stopband effect and open-stopband suppression.

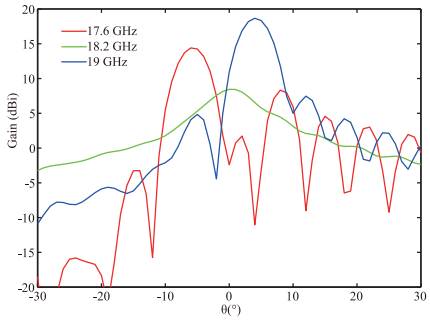

Fig. 4. Simulated radiation patterns with open-stopband effect.

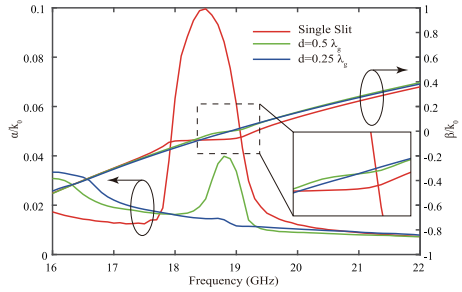

Fig. 5. Dispersion relations of the proposed HIS structure for various spacing d.

We can observe that at the broadside frequency, the gain drops significantly and the pattern has very serious distortion.

In order to mitigate the open-stopband effect, we add a secondary slit in each unit cell to cancel the reflected waves by the primary slit. Because the spacing between the primary and secondary slits is $\lambda_g/4$ and the round-trip phase equals π, the reflected waves by the primary and secondary slits have 180° phase difference between each other. The condition of forming destructive interference is satisfied for the reflected waves. Thus, the wave reflected by the secondary slit can nearly cancel the wave reflected by the primary slit. The solid lines presented in Fig. 3 show the S-parameters after the suppression of the open-stopband effect. In Fig. 5, a dispersion analysis is presented. From the figure, it can be observed that without the secondary slit, there is one obvious stopband region in the phase constant curve. Within this region, the attenuation constant shows a sharp increase. With the addition of the secondary slit and the spacing d gradually moving to $\lambda_g/4$, the stopband tends to be closed. The dispersion relations are extracted by using ANSYS HFSS.

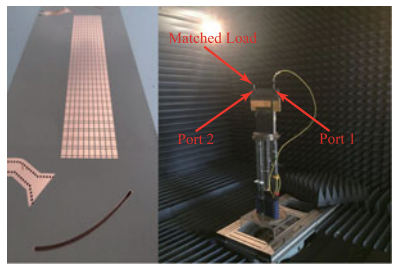

Fig. 6. Photographs of the fabricated antenna and measurement setup.

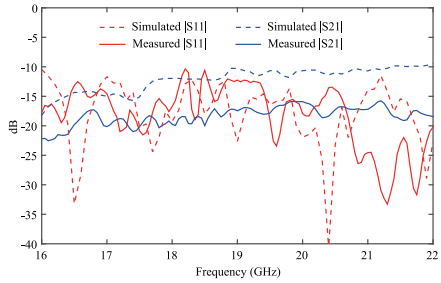

Fig. 7. Measured and simulated S-parameters of the prototype.

In the extraction process, we remove the two SWLs and place the proposed HIS structure (300 unit cells) in an airbox. The absorbing boundary condition is applied to the faces of the airbox. At the two ends of the HIS along the x-axis, two ports are assigned to act as the feed and load, respectively. The dispersion relations can be computed from the simulated S-parameters [12].

III. Experimental Demonstration and Discussion

The photographs of the fabricated antenna and measurement setup are presented in Fig. 6. Fig. 7 shows the measured and simulated magnitudes of S-parameters. It can be seen that the antenna shows good impedance matching from 16 to 22 GHz. The open-stopband effect is successfully suppressed. Compared to the simulation, the measured $|S_{21}|$ shows similar trend. However, in terms of values, it is almost 5 dB lower than the simulation. The radiation performance of the antenna prototype is measured in our compact range system, which simulates a far-field environment using a Mission Research Corporation blended rolled-edge reflector. The normalized measured backward and forward beams are compared to the simulated results in Fig. 8. From the figure, we can see that the measured radiation patterns show good agreements with the simulated beams on 3-dB beamwidth. For the backward beams, the sidelobes are below -11.5 dB. For the forward patterns, the side lobes at 21 and 22 GHz increase a little. It may be caused by the nonuniformity of the dielectric material. The broadside radiation performance at 19 GHz is investigated in Fig. 9. The measured and simulated results are compared.

The measured, simulated, and leaky-wave theory predicted beam angles and beamwidths are presented in Fig. 10. The predicted results are calculated by the approximate equations in [13] using the phase constant and attenuation constant presented in Fig. 5. The measured and simulated gains are presented in

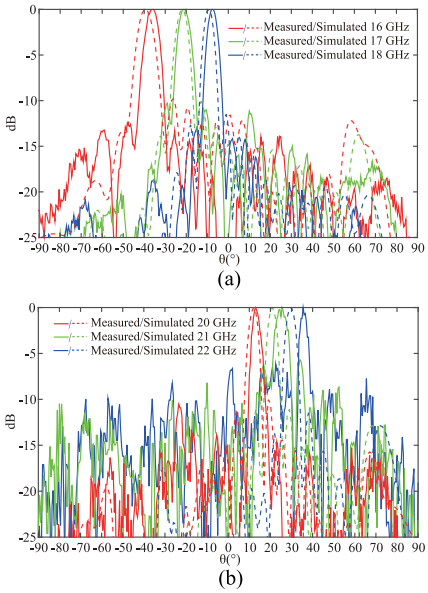

Fig. 8. Normalized measured and simulated (a) backward and (b) forward beams in the xz-plane for the proposed antenna.

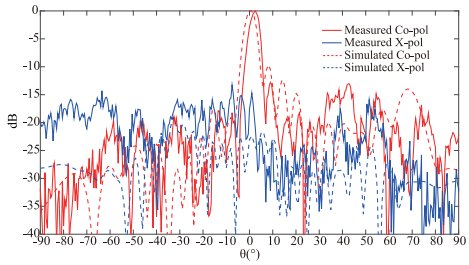

Fig. 9. Normalized measured and simulated broadside radiation patterns E_θ and E_ϕ in the xz-plane for the proposed antenna.

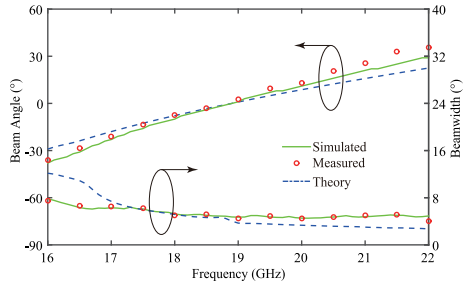

Fig. 10. Measured, simulated, and leaky-wave theory predicted main beam angles and beamwidths of the proposed antenna.

Fig. 11. We can see that the measured gain shows lower values than the simulation. The maximum discrepancy is almost 3.9 dB. For the measured results, the peak gain is 15.7 dBi at 16.5 GHz. The maximum gain variation within the frequency band is 2.5 dB. The developed antenna can realize frequency dominated beam scan from -36° to $+35.5^\circ$. It is worth mentioning that the differences between the simulated and the measured results may be caused by the imperfection of the dielectric substrate and some unavoidable fabrication tolerances. In the practical implementation, the used substrate may have higher permittivity and dissipation factor than those employed in ideal

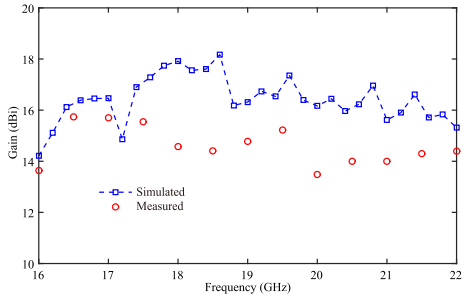

Fig. 11. Measured and simulated gain of the proposed antenna.

simulation. It will lead to discrepancies between measurement and simulation on the beam direction, $|S_{21}|$, and gain.

IV. Conclusion

In this letter, a collimated SW-excited HIS leaky-wave antenna has been proposed, designed, fabricated, and tested. The antenna can realize continuous beam steering with stable radiation pattern and gain from -36° to $+35.5^\circ$ within the frequency range 16–22 GHz. It can be a good candidate for radar systems and satellite communications.

References

[1] R. E. Collin and F. J. Zucker, *Antenna Theory*. New York, NY, USA: McGraw-Hill, 1969.

[2] A. R. Perkons, Y. Qian, and T. Itoh, "TM surface-wave power combining by a planar active-lens amplifier," *IEEE Trans. Microw. Theory Techn.*, vol. 46, no. 6, pp. 775–783, Jun. 1998.

[3] H. F. Hammad, Y. M. M. Antar, A. P. Freundorfer, and S. F. Mahmoud, "Uni-planar CPW-fed slot launchers for efficient TM_0 surface-wave excitation," *IEEE Trans. Microw. Theory Techn.*, vol. 51, no. 4, pp. 1234–1240, Apr. 2003.

[4] S. K. Podilchak, A. P. Freundorfer, and Y. M. M. Antar, "Surface-wave launchers for beam steering and application to planar leaky-wave antennas," *IEEE Trans. Antennas Propag.*, vol. 57, no. 2, pp. 355–363, Feb. 2009.

[5] S. K. Podilchak, L. Matekovits, A. P. Freundorfer, Y. M. M. Antar, and M. Orefice, "Controlled leaky-wave radiation from a planar configuration of width-modulated microstrip lines," *IEEE Trans. Antennas Propag.*, vol. 61, no. 10, pp. 4957–4972, Oct. 2013.

[6] X. Bai, S. W. Qu, K. B. Ng, and C. H. Chan, "Sinusoidally modulated leaky-wave antenna for millimeter-wave application," *IEEE Trans. Antennas Propag.*, vol. 64, no. 3, pp. 849–855, Mar. 2016.

[7] S. Paulotto, P. Baccarelli, F. Frezza, and D. R. Jackson, "A novel technique for open-stopband suppression in 1-D periodic printed leaky-wave antennas," *IEEE Trans. Antennas Propag.*, vol. 57, no. 7, pp. 1894–1906, Jul. 2009.

[8] J. T. Williams, P. Baccarelli, S. Paulotto, and D. R. Jackson, "1-D combline leaky-wave antenna with the open-stopband suppressed: Design considerations and comparisons with measurements," *IEEE Trans. Antennas Propag.*, vol. 61, no. 9, pp. 4484–4492, Sep. 2013.

[9] D. M. Pozar, "Microstrip antennas," *Proc. IEEE*, vol. 80, no. 1, pp. 79–91, Jan. 1992.

[10] A. W. Rudge and N. A. Adatia, "Offset parabolic-reflector antennas: A review," *Proc. IEEE*, vol. 66, no. 12, pp. 1592–1623, Dec. 1978.

[11] D. Deslandes and K. Wu, "Accurate modeling, wave mechanisms, and design considerations of a substrate integrated waveguide," *IEEE Trans. Microw. Theory Techn.*, vol. 54, no. 6, pp. 2516–2526, Jun. 2006.

[12] C. Caloz and T. Itoh, *Electromagnetic Metamaterials, Transmission Line Theory and Microwave Applications*. New York, NY, USA: Wiley, 2005.

[13] A. A. Oliner and D. R. Jackson, "Leaky-wave antennas," in *Antenna Engineering Handbook*, J. Volakis, Ed., 4th ed. New York, NY, USA: McGraw-Hill, 2007, ch. 10.